

# Numerical investigation of wind pressure coefficients on different scallop dome configurations

CAMILA C. GUERRA, MARCO D. DE CAMPOS

Institute of Exact and Earth Sciences  
Federal University of Mato Grosso,  
Av. Valdon Varjão, 6390, Barra do Garças, 78605-091, Mato Grosso  
BRAZIL

**Abstract:** The effects of the action of wind on scallop domes were numerically investigated using *Ansys* software, as well as the interference of the neighborhood on the external pressure coefficient and the streamlines between geometrically identical domes. The influence of the proportion on the neighborhood interference in scallop domes and the variations in the dimensions of the structures on the pressure coefficients and streamlines were also investigated. Five simulations were analysed involving six-grooved domes and geometric height variations for validation. The numerically obtained coefficients were compared with values in the literature. Other applications investigated the influence of grooves on the external pressure coefficient and the effect of wind on the grooved domes. Another application analysed the interference of the neighborhood on the external pressure coefficients and streamlines between three geometrically identical domes and, finally, the influence of the proportion in the study of the interference of the neighborhood. Here, the variations in the dimensions of the structure affected the pressure coefficients, and the streamlines were analysed. It was possible to verify the versatility and efficiency of the computational method used in the analysis of the action of wind.

**Key-Words:** Wind action, pressure coefficients, scallop domes, neighborhood effect, *Ansys*, computational method.

Received: July 23, 2021. Revised: April 17, 2022. Accepted: May 13, 2022. Published: June 1, 2022.

## 1 Introduction

Domes are complex in structural design due to their unique shape and efficiency in weakening elements such as wind [1]. In general, a dome is a curved roof structure that spans an area on a circular base, producing an equal thrust in all directions. They have a convex surface with double curvature, making them suitable for roofing, and can be built directly on the ground or on cylindrical walls. The wind loads considerably influence lightweight spatial structures with, for example, scallop domes with their various configurations and forms. The wind impact on a scallop dome is more complex due to its additional curvature.

Few studies approach the numerical simulation of wind in domes. Among the recent ones, Sadeghi, Heristchian, Aziminejad, and Nooshin [2] studied the effect of wind on grooved scallop domes and initially investigated the effect of wind on scallop domes to compare the consequence of grooves against the similar spherical dome. They concluded that the insertion of a slot into a spherical dome caused an abrupt change in its wind pressure coefficient in the vicinity of this slot. Sadeghi,

Heristchian, Aziminejad, and Nooshin [3] compared the numerical results with those obtained from the wind tunnel available in the literature. Then, numerically, the effect of structural flexibility and the neighborhood of the objects on the wind pressure distribution coefficients are studied. In another recent work, Fernandes and Campos [4] determined, via numerical simulation, the external pressure coefficients in vaulted buildings and analysed the action of the winds on a scallop dome located in a region where accidents due to wind occur. Sha, Zheng and Yue [5] investigated the interference effect on the wind load on two adjacent hemispherical dome structures. They concluded that the interference effect on the wind load on the two adjacent domes cannot be neglected and that a significant discrepancy exists under different incident wind directions when considering the influence of the adjacent dome. This influence is mainly the shielding effect by the upstream dome and the blocking effect by the downstream dome.

Rezaeinamdar, Sefid, and Nooshin [6] investigated the scallop dome and compared the results obtained from CFD with the corresponding

wind tunnel empirical data. They concluded that RANS models and the LES method could reasonably predict the front pressure coefficients for the range  $[0, \pm 90]$ . In the literature, dome arrangements have also been explored. For example, Tavakol, Yaghoubi, and Ahmadi [7] experimentally and numerically studied the flow around a series of domes, structures that, despite being widely used in the hot arid regions of the Middle East because of their ventilation advantages, have been little explored. They used wind tunnels for the experimental approach and simulation of large scales in the numerical implementation, exploring Reynolds numbers of 43,000 and 430,000. The results indicated that the separation points moved further downstream for the second and third domes compared with the first dome. Additionally, the peak suction pressure occurred near the apex of the first dome. Now, the maximum pressure occurred on the windward side of the third dome.

This work first compares and validates the results of the numerical CFD analysis with the literature. Then, using the CFD method, this paper investigates the effect of the neighborhood on the distribution of the external pressure coefficient. The streamlines between geometrically identical domes were also analysed.

## 2 Methodology

Numerical tests were performed using *Ansys Workbench* software, *fluid flow* module (CFX). The geometries were modelled with *AutoCAD* software and were composed of the structure to be analysed surrounded by the control volume, whose dimensions were adopted according to [2]: length of 4 m, width of 24 m and height of 2,6 m, with the dome centered inside it (Fig. 1). The wind direction considered was  $0^\circ$  concerning the domes, and the wind speed adopted was 38 m/s.

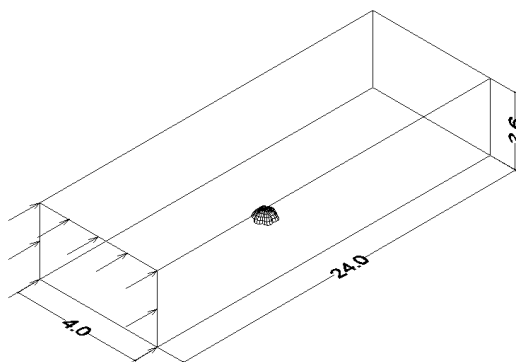


Fig. 1 Volume control

## 3 Numerical applications

**Case 1:** Here, to validate the methodology, the scallop domes were adopted with 6 grooves with variations in the height of the geometry, adopting the aspect ratio given by  $k=h/D$  and the relationship between height ( $h$ ) and diameter ( $D$ ) fixed at 50 cm. Considering the two decimal place precision, for  $k=0,1$ , the greatest difference (24%) occurred between the first boundary, starting from the outer edge to the inner line of the dome. The same occurred for the domes with  $k=0,2$ . In the scallops domes with six grooves and  $k=0,3; \dots; 0,5$ , the values for the  $C_{pe}$  contours were similar (Tab. 1) when compared to those presented by [2]. However, for  $k=0,4$  and  $k=0,5$ , at the top of the geometry crest, an area of the larger contour can be observed, which has a high aspect ratio and, consequently, presents the highest  $C_{pe}$  values. Compared with [2], differences of 17% and 13% were obtained for the maximum and minimum pressure coefficients, respectively. According to [2], with the increase in the aspect ratio of the dome, the lengths of its grooved parts decrease, especially in the grooves at  $90^\circ$  concerning the wind direction, due to the type of cutout of this dome. In this way, with the increase in the aspect ratio, the suction effect of the critical groove was increased; for example,  $C_{pe_{min}} = -0,88$  for  $k=0,3$  and  $C_{pe_{min}} = -1,31$  for  $k=0,5$  were obtained.

**Case 2:** In this case, wind pressure coefficients in three distinct dome scenarios with various aspect ratios are studied. All domes have the same diameter, varying their elevation, denoted by  $h$ , from  $0,1D$  to  $0,5D$ , with  $D$  being its diameter. The three situations analysed, different by the number of grooves in each geometry (10, 14, and 25), aim to investigate the influence of the grooves on the wind behavior and, consequently, on the pressure coefficients. Initially, the wind action was simulated in domes with 10 grooves, with a  $0^\circ$  wind direction. The pressure coefficients obtained, as well as the pressure contour lines, can be seen in Fig. 2(a). It was found that as the aspect ratio was increased, there was an increase in the external pressure coefficient. A significant suction area to leeward was also noted, especially in the domes with  $k = 0,3; \dots; 0,5$ , and for these, it was noted that the module higher values of the pressure coefficient, they are directed to the grooved sections between  $36^\circ$  and  $108^\circ$  concerning the wind direction and, similarly, in the grooves between  $252^\circ$  and  $324^\circ$ , thus evidencing the increase in the indentations represented by the contour lines. Additionally,  $C_{pe_{min}}$  for  $k=0,4$  and  $k = 0,5$  occurred in the groove at  $72^\circ$  and  $288^\circ$  for the wind, and this suction was relieved at the top and lee side of the geometries. To

Table 1. External pressure coefficients of the scallop dome with six grooves considering  $k = 0.1; \dots; 0.5$

$k = 0,1$									
Sadeghi <i>et al.</i> [2]			+0,25		+0,00		-0,25		
Present work			+0,19		-0,02		-0,24		
Difference			0,06		0,02		0,01		
$k = 0,2$									
Sadeghi <i>et al.</i> [2]	+0,50		+0,25		+0,00		-0,25		-0,50
Present work	+0,40		+0,19		-0,02		-0,24		-0,45
Difference	0,10		0,06		0,02		0,01		0,05
									0,08
$k = 0,3$									
Sadeghi <i>et al.</i> [2]	+0,75	+0,50	+0,25	+0,00	-0,25	-0,50	-0,75	-1,00	
Present work	+0,62	+0,40	+0,19	-0,02	-0,24	-0,45	-0,67	-0,88	
Difference	0,13	0,10	0,06	0,02	0,01	0,05	0,08	0,12	0,12
$k = 0,4$									
Sadeghi <i>et al.</i> [2]	+0,75	+0,50	+0,25	+0,00	-0,25	-0,50	-0,75	-1,00	-1,24
Present work	+0,62	+0,40	+0,19	-0,02	-0,24	-0,45	-0,67	-0,88	-1,09
Difference	0,13	0,10	0,06	0,02	0,01	0,05	0,08	0,12	0,15
$k = 0,5$									
Sadeghi <i>et al.</i> [2]	+0,75	+0,50	+0,25	+0,00	-0,25	-0,50	-0,75	-1,00	-1,24
Present work	+0,62	+0,40	+0,19	-0,02	-0,24	-0,45	-0,67	-0,88	-1,09
Difference	0,13	0,10	0,06	0,02	0,01	0,05	0,08	0,12	0,15

the windward side, it was observed that  $Cpe_{max}$  occurred in the frontal part of the domes configured with an aspect ratio greater than 0,3. For the domes with 14 grooves, the same geometric parameters previously adopted were maintained. Figure 2(b) shows the pressure coefficients and isobaric lines as well as the pressure distribution on the external surface of the domes. It was noted that the isobaric lines behaved similarly to the previous case, in which the domes had 10 grooves; however, with the increase in grooves and, consequently, in the number of geometry sections, there was an increase in indentations, and these, in turn, were predominantly located at  $51^\circ$  and  $77^\circ$ .

Compared with the 10-groove geometries, a decrease in the external pressure coefficients was noted. For cases with 14 grooves, the increase in the number of grooved sections influenced the result of the coefficients. Finally, five situations were simulated with the same aspect ratio variations for the domes with 25 grooves (Fig. 1(c)), and a significant difference was observed in the results obtained for the external pressure coefficients when compared to the cases with 10 and 14 grooves. A 23% reduction in  $Cpe_{min}$  was noted with the 14-slotted geometry and 26% with the 10-slotted domes. An increase in indentations was noted for the case with 25 grooves (Fig. 1(c)), demonstrating the tendency of the module highest coefficients to be directed towards the sections delimited by the grooves. For  $k=0,5$ ,  $Cpe_{min}$  was concentrated on sections between  $58^\circ$  and  $86^\circ$  for the wind direction

and, similarly, on grooves between  $302^\circ$  and  $331^\circ$ , in addition to converging to the crest of this geometry. When comparing the cases with 10, 14, and 25 grooves, it was noted that the wind behaved similarly, and the maximum and minimum coefficients were concentrated in the same regions, with the maximum in the windward sections and the minimum at the top and sides of geometries. As the number of grooves was increased, a decrease in pressure coefficients was noticed, showing the influence of the grooves. Therefore, the dome with 25 grooves presented a better performance regarding the minimum external pressure coefficient and was chosen for Case 3.

**Case 3:** The distribution of wind pressure distribution on an object is not only a function of its shape but is also a function of the effect of the nearby objects, according to [3]. Thus, this effect was studied, as well as the Venturi effect and the blowing effect on the external pressure coefficient between the cups. The domes were named *A*, *B*, and *C*, with *A* and *B* being the source of interference and dome *C* referred to as the reference dome (Fig. 3(a)). All have 25 grooves and ratio  $k=0,5$  and were positioned at a distance  $L$ , which varies in the range  $[0;2D]$ , measured from their outer edge, where  $D$  is the diameter of the dome. To calculate the wind speed along the control volume, 38 m/s was adopted for the basic speed. The neighborhood effect tends to decrease with increasing distance between them. Thus, for  $L=0,25D$  and  $L=0,5D$ , a smaller influence

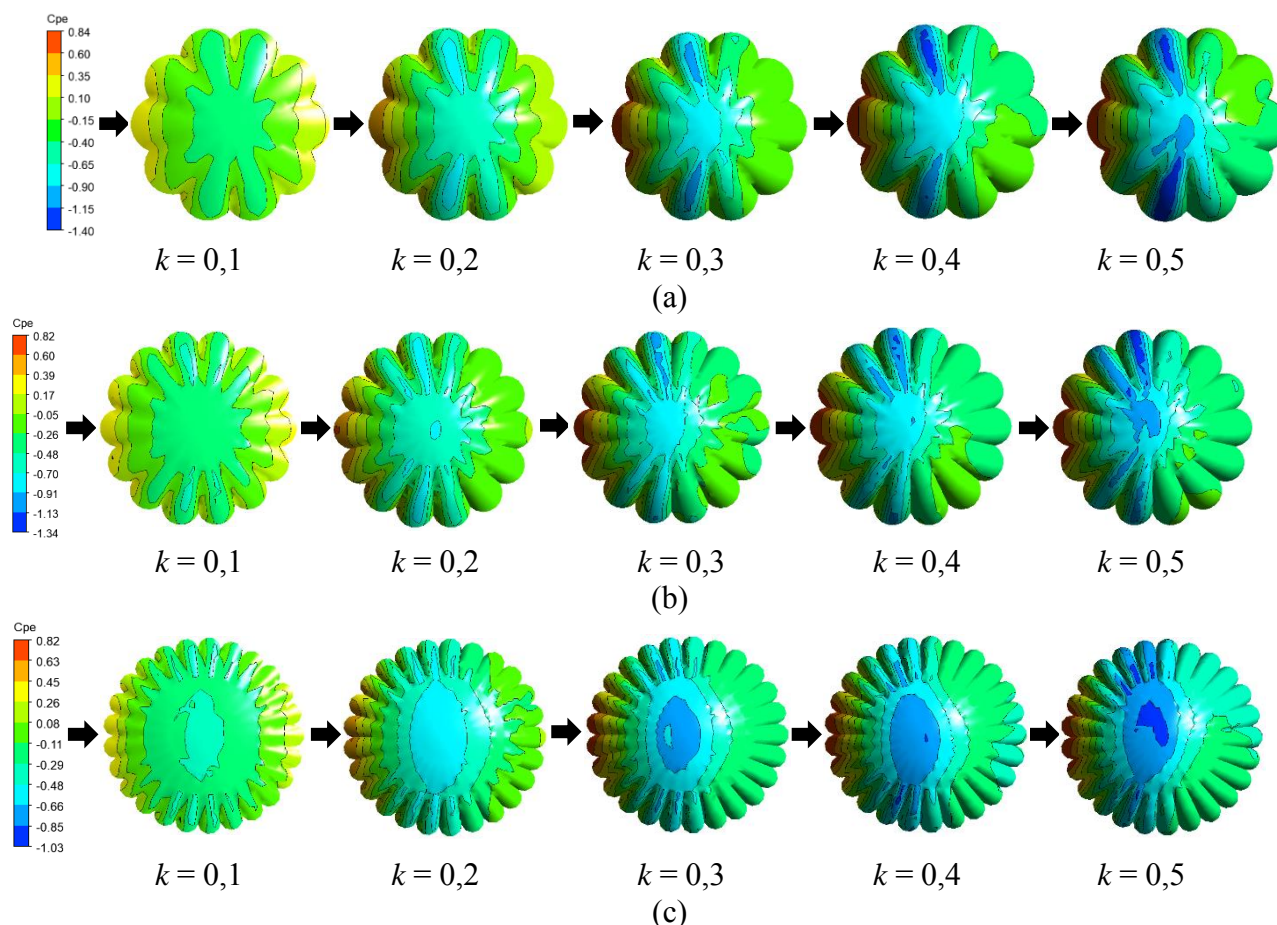


Fig. 2 Variation of external pressure coefficients on scallop domes with (a) 10 grooves, (b) 14 grooves, (c) 25 grooves and different aspect ratios

of the interference domes  $A$  and  $B$  on the reference dome  $C$  was noticed. In addition, there was an increase in the flow velocity caused by the bottleneck in flow between geometries  $A$  and  $B$ , making the external pressure coefficients higher on the surfaces where the taper occurred (Fig. 3(b-c)). Vortex shedding became more evident from the set  $L=0,25D$ , and consequently, the blowing effect caused by the interference domes became more active. This dynamic effect generated by wind turbulence from structures  $A$  and  $B$  caused changes in pressure, causing the  $C_{pe}$  of reference dome  $C$  to increase. For the last two simulations,  $L=D$  and  $L=2D$  were adopted, there was a small interference from the neighborhood, and the values of the external pressure coefficients were similar to those found in the previous case. In the  $L=D$  configuration, domes  $A$  and  $B$  had no interference from the neighborhood, while dome  $C$  had a small decrease in the  $C_{pe_{max}}$  region. Furthermore, there was no change in the values of the pressure coefficients, and the wind taper started to decrease and, consequently, the interference of the effects on the structures (Fig. 3(e)). As the value of  $L$

increases, the areas of overpressure in the reference domes also increase. Furthermore, the critical suction range tends to increase in these domes, and for  $L=2D$ , a wider area is reached with the highest suction, different from those with low values of  $L$ , which suffer from the shielding effect of the domes of interference  $A$  and  $B$  (Fig. 3(f)). It was noted that for the distance  $L=2D$ , the external pressure coefficients remained the same as in the previous case considering 25 grooves and the ratio  $k=0,5$ , unlike the domes spaced at  $L < D$ , which suffered directly from the effects caused by the presence of the neighborhood. Concerning the wind speed in the simulations, a percentage increase of approximately 21% was observed for the basic speed, especially in areas where the bottleneck in the wind caused by the proximity of the structures occurred, reaching approximately 46 m/s, making the external pressure coefficients larger on these surfaces.

**Case 4:** In this case, two 25-grooved scallop domes were studied to verify the influence of proportion in the study of neighborhood interference. The same aspect ratio as in the previous case was adopted,

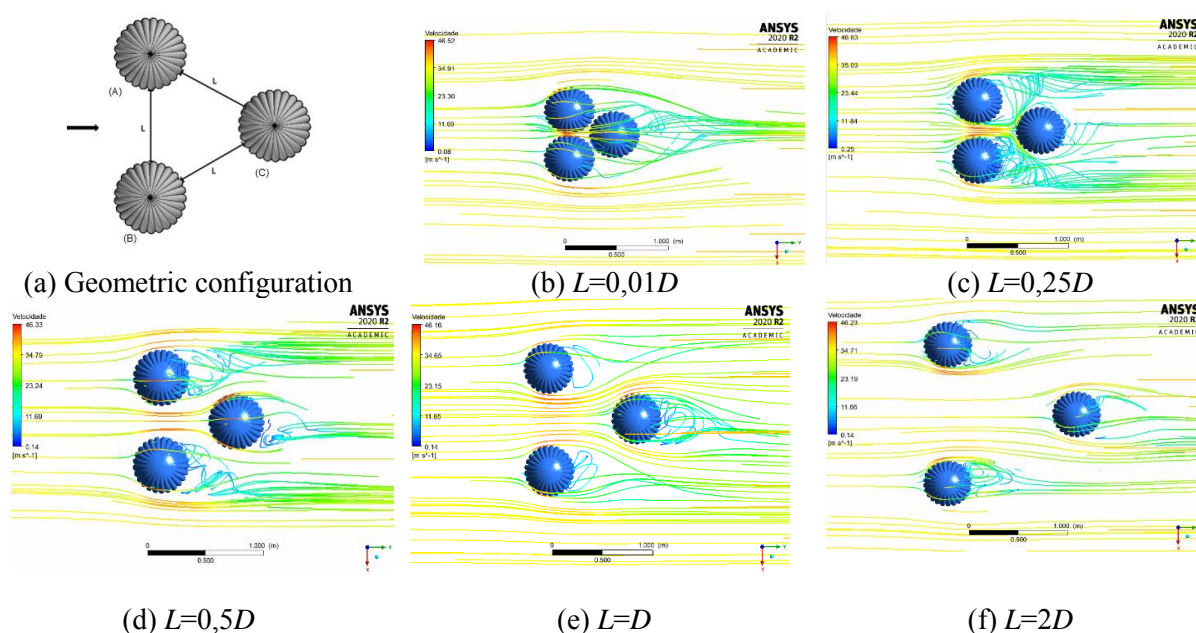


Fig. 3 Geometric configuration and variation of external pressure coefficients and the streamlines with respect to the arrangement of three scallop domes with 25 grooves and  $k=0,5$ .

varying the diameter, height, and distance of the domes. According to the previous case, there was a greater influence of the neighborhood when  $L \leq D$ , and consequently, in the first two simulations, the applications. The external pressure coefficients and current lines for these profiles are shown in Fig. 4(a-b). Adopting these same distances, there was no discrepancy in the results when compared to the values obtained in the previous case, and the isobaric lines and the current lines were distributed similarly, with a change of 9% in the first simulation and 3% in the second simulation for the minimum external pressure coefficient. In the third and fourth simulations (Fig. 4(c-d)), a diameter of  $4/5D$  was adopted for the interference domes, and the value of  $D$  was fixed for the reference dome. The distances used were  $L=0,5D$  and  $L=0,25D$ , respectively. The results for the third simulation showed a reduction, in module, of 11% of the  $Cpe_{min}$  when compared to the case with the same distance between the domes, demonstrating the tendency of attenuation of the suction values according to the reduction in the proportion of the domes of interference. It was also verified that this same pressure coefficient in the module increased as the distance between the structures decreased, as observed in the fourth simulation (Fig. 4(d)), contrary to what occurred in the first two simulations, in which  $Cpe_{min}$  declined with the proximity of the domes. The  $Cpe_{min}$ , in turn, increased as the structures approached due to the “funneling” of the wind caused by the interference domes. For the last simulation,  $L=0,25D$  was adopted. One of the interference domes was

distance was adopted as  $L = D$  and  $L = 0,5D$ . The diameter of the interference domes was fixed at  $D = 0,5$  m, and for the reference dome, the value of  $D'=4/5D$  was assumed in both designed with a diameter equal to  $D$ , while the other interference geometry and the reference dome were configured with  $D'=4/5D$  (Fig. 4(e)). As in other simulations involving neighborhoods, it was found that the minimum pressure coefficient of the interference domes to leeward in the module was greater than that of the reference domes due to the mat formed between the geometries. In general, in the simulations of this case, there were no significant changes in the pressure coefficients or the distribution of the streamlines compared to the previous case. However, in the domes with  $4/5D$ , as the distance from the other buildings was made, the pressure coefficient in the module was reduced as a result of the decrease in the proportions of the geometry. Nevertheless, the reduction pressure coefficient was not significant. In turn, the diameter domes  $D$  showed results similar to the previous case.

## 4 Conclusions

In the first case, five applications involving scallop domes with six grooves and with variations in the height of the geometry, the coefficients obtained numerically were compared with the literature for validation. The pressure coefficients presented differences concerning the literature, on the order of 13% and 17%, for the minimum and maximum pressure coefficients, respectively. In the second

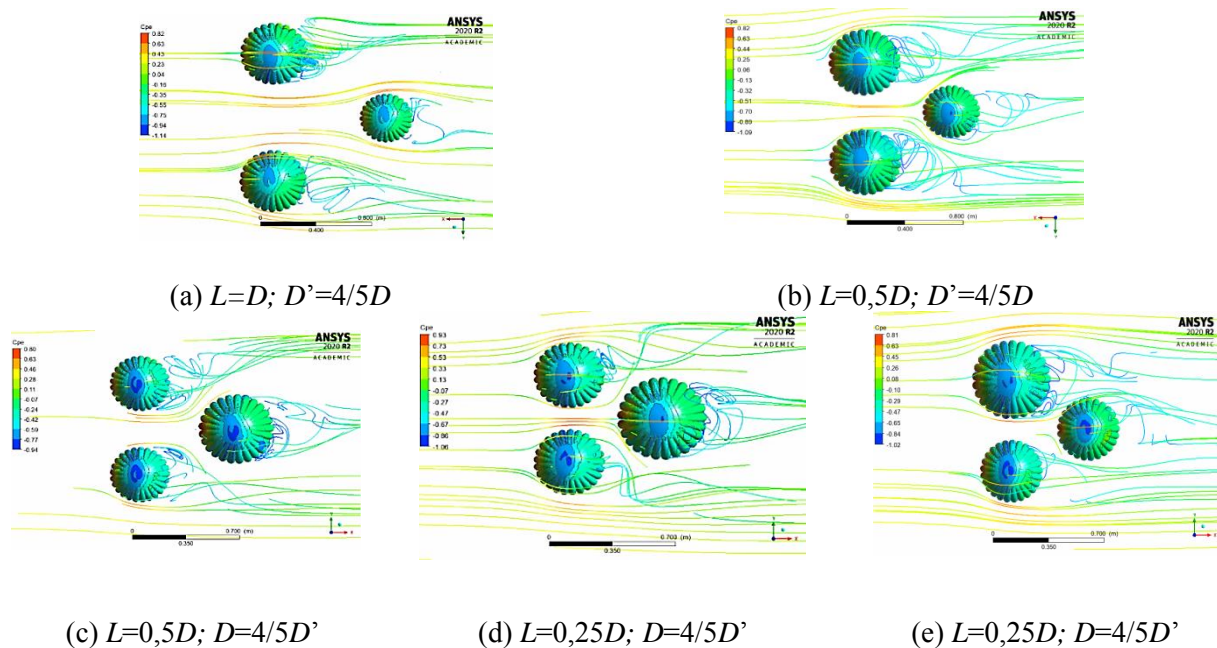


Fig. 4 Variation in the external pressure coefficients and streamlines with respect to the arrangement of three scallop domes with 25 grooves and  $k=0,5$ .

case, the influence of the grooves on the external pressure coefficient and the wind distribution in the structure was investigated considering domes with 10, 14, and 25 grooves. A decrease in the pressure pressure coefficient and the current lines between three domes with identical geometric characteristics, with 25 grooves, and the ratio  $k=0,5$  was analysed. The results showed that the wind action caused changes in pressures and current lines in the vicinity of the structures, especially when  $L < D$ , and they became almost null from  $L=2D$ . For the wind speed, there was a percentage increase of approximately 21% concerning the adopted basic speed, seen, above all, in the areas of "tapering" of the wind caused by the proximity between the structures, causing an increase in the external pressure coefficients in these areas. In the last case, the influence of proportion in the study of neighborhood interference for domes with 25 slots and ratio  $k = 0.5$  was investigated, as well as the effect of variations in structure dimensions on pressure coefficients and streamlines. It can be noted that for this configuration, compared to the previous case, the pressure coefficients and the distribution of the current lines did not show significant changes less than the  $4/5 D$  domes, which, as the distance of the buildings, the pressure coefficient in the module was reduced.

Although some contours presented errors in the range of 20% to 30% to the literature, Ferziger (1990) points out that lower accuracies, with errors above 25%, can be admitted in Wind Engineering.

coefficients was observed as the number of grooves was increased, proving the influence of the grooves on the coefficients. In the third case, the interference of the neighborhood on the external

In future works, other configurations and arrangements involving scallop domes could be studied, as well as the calculation of the internal pressure.

#### References:

- [1] R. L. C. Canlas, M. T. J. N. Principe, G. S. Riego and V. E. DyReyes, Finite Element Analysis on a single-story geodesic dome structure using combination of Po-Lite Hollow Blocks and Cold-Formed Steel. In: *TENCON 2021 - 2021 IEEE Region 10 Conference (TENCON)*, 2021, pp. 816-820.
- [2] H. Sadeghi, M. Heristchian, A. Aziminejad and H. Nooshin, Wind effect on grooved and scallop dome, *Engineering Structures*, Vol. 148, 2017, pp. 436-450.
- [3] H. Sadeghi, M. Heristchian, A. Aziminejad and H. Nooshin, CFD simulation of hemispherical domes: structural flexibility and interference factors, *Asian Journal of Civil Engineering*, Vol. 19, No. 5, 2018, pp. 535-551.
- [4] K. K. B. Fernandes and M. D. Campos, The effects of external wind pressure distributions on grooved and scallop domes. In: *Congress on Scientific Researches and Recent Trends-VIII*, 2021, Zambales. Full Text Book. IKSAD Global Publications, 2021, pp. 281-295.

- [5] W. Sha, D. Zheng and J. Yue, Experimental study on the interference effect of wind load on two adjacent hemispherical domes. In: *IEEE International Conference on Artificial Intelligence and Information Systems*, 2020, Dalian. Proceedings. Institute of Electrical and Electronics Engineers (IEEE), 2020, pp. 757-761.
- [6] F. Rezaeinamdar, M. Sefid and H. Nooshin, Numerical and experimental investigation of wind pressure coefficients on scallop dome, *International Journal of Optimization in Civil Engineering*, Vol. 12, No. 3, 2022, pp. 313-334.
- [7] M. M. Tavakol, M. Yaghoubi and G. Ahmadi, Experimental and numerical analysis of airflow around a building model with an array of domes, *Journal of Building Engineering*, Vol. 34, 2021, 101901.
- [8] J. H. Ferziger, Approaches to turbulent flow computation: applications to flow over obstacles, *Journal of Wind Engineering and Industrial Aerodynamics*, Vol. 35, 1990, pp. 1-19.

### **Contribution of individual authors to the creation of a scientific article**

Camila Guerra was responsible for the methodology and carried out the simulation and writing. Marco Campos carried out the conceptualization; writing, review and editing.

### **Creative Commons Attribution License 4.0 (Attribution 4.0 International , CC BY 4.0)**

This article is published under the terms of the Creative Commons Attribution Licence 4.0

[https://creativecommons.org/licenses/by/4.0/deed.en\\_US](https://creativecommons.org/licenses/by/4.0/deed.en_US)